Doping-dependent superconducting gap anisotropy in the two-dimensional pnictide Ca_{10}(Pt_{3}As_{8})[(Fe_{1-x}Pt_{x})_{2}As_{2}]_{5}

K. Cho, M. A. Tanatar, H. Kim, W. E. Straszheim, N. Ni, R. J. Cava, and R. Prozorov

Doping - dependent anisotropic superconducting gap in the triclinic pnictide $\mathbf{Ca_{10}(Pt_3As_8)[(Fe_{1-x}Pt_x)_2As_2]_5}$

K. Cho,[1] M. A. Tanatar,[1] H. Kim,[1, 2] W. E. Straszheim,[1] N. Ni,[3] R. J. Cava,[3] and R. Prozorov[1, 2, *]

[1] *The Ames Laboratory, Ames, IA 50011, USA*
[2] *Department of Physics and Astronomy, Iowa State University, Ames, IA 50011, USA*
[3] *Department of Chemistry, Princeton University, Princeton, NJ 08544, USA*

The characteristic features of $Ca_{10}(Pt_3As_8)[(Fe_{1-x}Pt_x)_2As_2]_5$ (the "10-3-8" phase) superconductor are triclinic symmetry, high anisotropy and a clear separation of superconducting and antiferromagnetic regions in the T vs. doping (x) phase diagram, which allows studying the superconducting gap without complications due to the coexisting magnetic order. The London penetration depth, measured on the underdoped side of the superconducting "dome" ($x = 0.028$, 0.041, 0.042, and 0.097), shows behavior remarkably similar to other Fe-based superconductors, exhibiting a robust power-law, $\Delta\lambda(T) = AT^n$. The exponent n decreases from 2.36 ($x = 0.097$, close to the optimal doping) to 1.7 ($x = 0.028$, a heavily underdoped composition), suggesting that the superconducting gap becomes more anisotropic at the dome edge. A similar trend is found in the lower anisotropy $BaFe_2As_2$ ("122") - based superconductors, implying that it is an intrinsic property, unrelated to the coexistence of magnetic order and superconductivity or the anisotropy of the normal state.

Recently a new family of Fe-based superconductors (FeSCs) with PtAs intermediary layers has been reported in a Ca-Fe-Pt-As system [1]. In particular, $Ca_{10}(Pt_nAs_8)[(Fe_{1-x}Pt_x)_2As_2]_5$ with n = 3 (the "10-3-8" phase) and n = 4 (the "10-4-8" phase) have been described [2–5]. Whereas the 10-3-8 phase with triclinic symmetry (which is rare in superconductors) shows superconducting T_c up to 13 K upon Pt-doping, the superconductivity of a tetragonal 10-4-8, stabilizes at a higher T_c of 38 K [2]. The availability of high purity single crystals with well - controlled level of Pt doping makes the 10-3-8 system particularly attractive [2–5]. Two unique features distinguish the 10-3-8 system from other FeSCs. First, the anisotropy of the 10-3-8 system, $\gamma_H(T_c) \equiv H(T_c)_{c2,ab}/H(T_c)_{c2,c} \sim 10$ [3], is much larger than $2-4$ in the 122 systems and even larger than $7-8$ in the 1111 systems [6–8]. Second, a clear separation of structural (magnetic) instability and superconductivity in the $T(x)$ phase diagram, suggested by transport measurements [3] and supported by our direct imaging of structural domains shown in Fig. 1. This is distinctly different from the 122 pnictides, where these two order parameters coexist up to the optimal doping [9].

In the cuprates, the low dimensionality of the electronic structure is believed to be responsible for their high T_c and highly anisotropic gap (d-wave) [10]. Despite obviously layered structure, the electronic anisotropy of most - studied 122 pnictides is rather low, with $\gamma_H(T) \sim 2-4$ at $T = T_c$ and decreasing upon cooling [6–8]. Moreover, the superconducting gap in the 122 pnictides is rather isotropic at the optimal doping, but evolves towards nodal structure at the dome edges [11]. To check whether the electronic anisotropy plays a role in the structure of the superconducting gap, highly anisotropic pnictides without complications due to coexisting phases and well - controlled doping level are needed and the 10-3-8 system fits these requirements.

In this work, we studied the 10-3-8 crystals in the underdoped regime up to optimal doping. The low-temperature penetration depth exhibits power-law variation, $\Delta\lambda = AT^n$, with the exponent n decreasing towards the edge of the dome. This behavior is similar to the lower-anisotropy BaK122 (hole doped) [12] and BaCo122 (electron doped)[13]. We conclude that neither the anisotropy (at least, up to $\gamma_H \sim 10$) nor the coexistence of superconductivity and magnetism play a significant role in determining the superconducting gap structure in FeSCs.

Single crystals of $Ca_{10}(Pt_3As_8)((Fe_{1-x}Pt_x)_2As_2)_5$ were synthesized as described elsewhere [3]. The compositions of six samples were determined with wavelength dispersive spectroscopy (WDS) electron probe microanalysis as $x = 0.004\pm0.002$, 0.018 ± 0.002, 0.028 ± 0.003, 0.041 ± 0.002, 0.042 ± 0.002, and 0.097 ± 0.002. The in-plane London penetration depth, $\lambda(T)$, was measured using a self-oscillating tunnel-diode resonator (TDR) technique [14–16]. The sample was placed with its c-axis along the direction of ac-field, H_{ac}, induced by the inductor coil. Details of the measurements and calibration can be found elsewhere [14]. Polarized light imaging of the structural domains, shown in Fig. 1, was done with a Leica microscope in a flow-type optical ^{4}He cryostat, for details see [9, 17].

Figure 1 shows polarized-light optical images for two samples with different compositions, practically undoped, $x = 0.004$ (top panel - at 5 K, and middle panel - at 95 K), and superconducting ($T_c \sim 6$ K) heavily underdoped, $x = 0.028$ (lower panel, at 5 K). The mesh-like contrast clearly visible in the top panel is due to the formation of structural domains. The polarization plane rotates differently upon reflection from the neighboring twins, thus resulting in a difference in the light contrast as observed through an analyzer. Usually, such domains are formed upon lowering the symmetry of the lattice. In
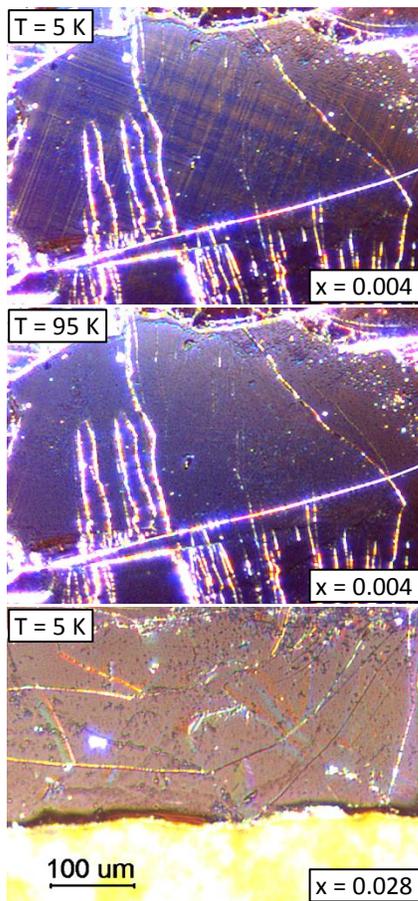
FIG. 1. (Color online) Polarized-light images of single crystals of the 10-3-8 system with $x = 0.004$ at 5 K showing a clear twin-domain pattern below the transition (top), and at 95 K with no domains above the transition (middle). The most underdoped superconducting composition, $x = 0.028$, does not show any domains down to 5 K (bottom).
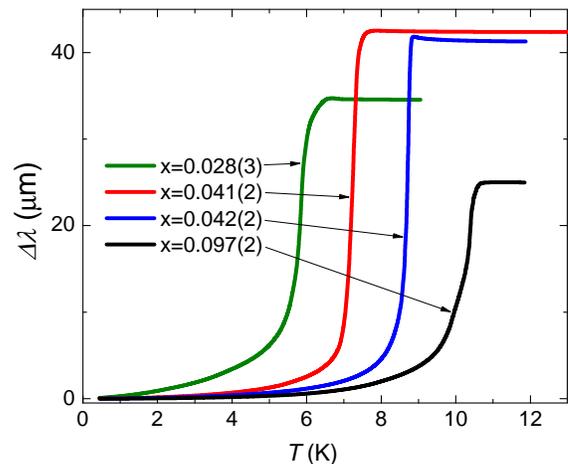

FIG. 2. (Color online) Variation of the London penetration depth, $\Delta\lambda(T)$, in the full temperature range for four underdoped compositions of the 10-3-8 system. T_c increases with Pt-doping, x, as indicated in the legend.

most pnictides this is a transition from the tetragonal to the orthorhombic phase and is also accompanied by an antiferromagnetic transition [9, 17]. In the present case, we already start with the lowest symmetry triclinic system and the only possibility to form domains is to have another transition that would cause additional stress. More information on structural domains in triclinic systems can be found elsewhere [18]. The long-range antiferromagnetic ordering would cause such stresses, via magnetostrictive coupling, which is very pronounced in the pnictides. In the composition with $x = 0.004$, the present observation of domains coincides with the feature ($T_s \sim 90$ K) observed in the resistivity on samples from same batch [19]. Note that despite its triclinic crystal structure, a four-fold symmetry of the electronic structure was found in angle resolved photoemission spectroscopy (ARPES) [5], suggesting that triclinic distortion plays a minor role in determining the band - structure. In the same ARPES study, however, the authors didn't

rule out the possibility that the four-fold symmetry can only occur on the surface, not in the bulk, due to subtle surface reconstruction. The lower panel in Fig. 1 shows the most underdoped 10-3-8 superconducting composition with $x = 0.028$ imaged at 5 K. We do not observe any domains and the picture does not change at room temperature. In addition, the resistivity of $x = 0.028$ composition ($x_{EDS} = 0.07$ in Ref. [3]) does not show any features suggesting structural phase transition. While the compositions with $x = 0.004$ ($T_s \sim 90$ K) [19] and $x = 0.018$ ($T_s \sim 50$ K, $x_{EDS} = 0.06$ in Ref. [3]) do not show superconductivity, the composition with $x = 0.028$ has $T_c \sim 6$ K, but no T_s. From this comparison, we conclude that the domains of magnetic and superconducting orders are clearly separated in the $T(x)$ phase diagram in the 10-3-8 system (see Fig. 4 (c) below).

Figure 2 shows the variation of the London penetration depth, $\Delta\lambda(T)$, during a temperature sweep through the superconducting transition in 10-3-8 single crystals with $x = 0.028$, 0.041, 0.042, and 0.097. T_c monotonically increases with x, consistent with the transport measurements of the crystals from the same batches [3].

Figure 3 shows $\Delta\lambda(T)$ plotted against (a) linear, T/T_c, and (b) quadratic, $(T/T_c)^2$, normalized temperature scales. For the quantitative analysis, $\Delta\lambda(T)$ was fitted to a power-law, $\Delta\lambda(T) = AT^n$. To examine the robustness of the fits, the fitting range was varied from base temperature to $T_c/3$, $T_c/4$, and $T_c/5$ (indicated by vertical dashed lines in Fig. 3). In Fig. 3, the symbols are experimental data and the solid lines show representative fits with the upper limit of $T_c/3$. The resulting exponents n for all three fitting ranges are shown in Fig. 4 (a). Figure 4 (b) shows the prefactor A obtained at a fixed $n = 2$ for different fitting ranges. To compare samples with different doping levels we used the average values
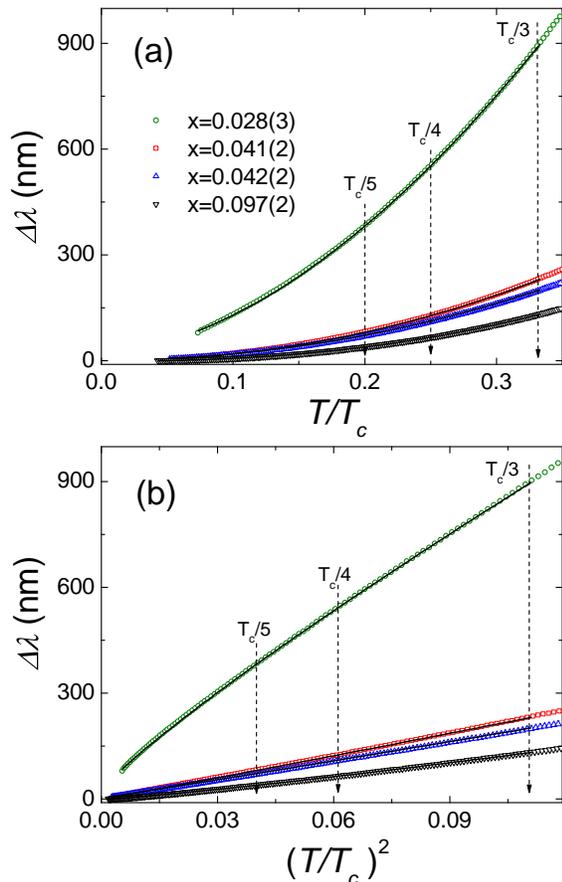
FIG. 3. (Color online) $\Delta\lambda(T)$, plotted against (a) T/T_c and (b) $(T/T_c)^2$ for the 10-3-8 samples with $x = 0.028$, 0.041, 0.042, and 0.097. The vertical dashed lines indicate the upper limits of the fitting ranges, $T_c/5$, $T_c/4$ and $T_c/3$. The solid lines are representative fits to $\Delta\lambda = AT^n$ for each doping, conducted with the upper limit of $T_c/3$. The resulting exponents n for all three fitting ranges are shown in Fig. 4 (a).
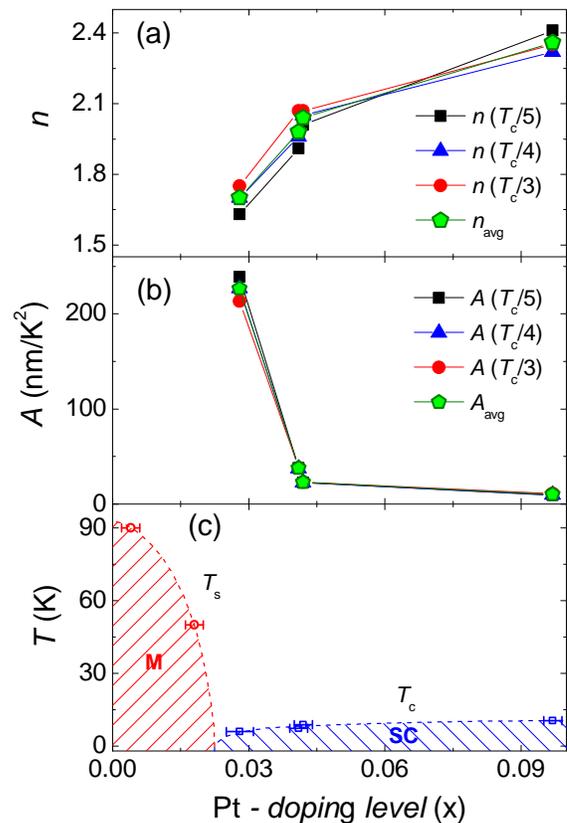
FIG. 4. (Color online) Results of the power-law fits with three different upper limits, indicated by dashed lines in Fig. 3 are shown along with the average values. Panel (a): the exponent n, obtained by keeping A and n as free parameters. Panel (b): the pre-factor A, obtained at a fixed $n = 2$. Panel (c) shows the doping phase diagram with the magnetic (M) and superconducting (SC) phases clearly separated as a function of Pt-doping (x). T_s measured from resistivity [3, 19] and T_c from TDR (this work).

(over three different fitting ranges), n_{avg} and A_{avg}.

As shown in Fig. 4 (a), n_{avg} decreases from 2.36 to 1.7 and the prefactor, A, dramatically increases (fivefold) as x decreases from nearly optimal doping of $x = 0.097$ towards heavily underdoped $x = 0.028$. This behavior signifies a much larger density of quasiparticles thermally excited over the gap minima in the underdoped compositions.

A similar doping-dependent evolution of $\lambda(T)$ was found in BaCo122 [13]. For that compound, it was suggested that the underdoped side is significantly affected by the co-existing magnetic order and was explained by an increasing gap anisotropy when moving towards the edge of the "superconducting dome", consistent with thermal conductivity [20, 21] and specific heat [22] studies. In the present case of the 10-3-8 system where magnetism and superconductivity are separated, Fig. 4 (c), this doping-dependent evolution of n and A suggests that

the development of the anisotropy of the superconducting gap upon departure from the optimal doping is a universal intrinsic feature of iron-pnictides, and is not directly related to the coexistence of magnetism and superconductivity.

The low-temperature exponent n, is sensitive to the gap anisotropy, but does not reflect possible multi-gap structure typical for the pnictides [11]. Therefore we need to analyze the superfluid density in the full temperature range. To avoid complications due to anisotropy we perform this analysis at the optimal doping. Figure 5 shows the superfluid density, $\rho_s(T) = (\lambda(0)/\lambda(T))^2$, calculated with $\lambda(0)$ of 200 nm and 500 nm, representing two extreme values reported for the pnictides [23]. Clearly, single-gap d-wave and s-wave are very far from the data. A much better agreement was found by using a self-consistent two-gap (s-wave) γ model [24], which only deviates at the low temperatures, presumably due to pairbreaking scattering [25]. The ratio of the superconducting gaps is
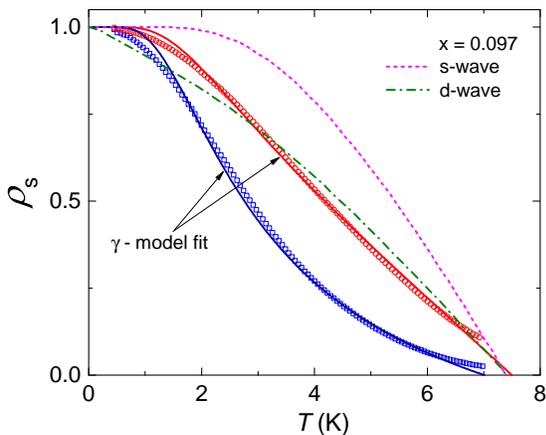
FIG. 5. (Color online) Superfluid densities, $\rho_s(T)$, of the optimally doped 10-3-8 sample with $x = 0.097$ for $\lambda(0) = 200$ nm (squares) and 500 nm (circles), which cover extremes of $\lambda(0)$ in FeSCs. Solid lines are the fits from the two-gap (s-wave) γ model [24]. For comparison, $\rho_s(T)$ for single-gap s-, and d-wave cases are shown as dashed lines.

about 2, similar to other FeSCs.

To summarize our findings, we observe substantial increase of the gap anisotropy in more underdoped compositions of the 10-3-8 system despite a clear separation of superconducting and magnetic domains on the $T(x)$ phase diagram. Interestingly, similar separation is also reported in the 1111 compounds that have similarly high electronic anisotropy [26, 27]. The evolution of the gap anisotropy with doping may signify a transition between different pairing mechanisms in the different parts of the superconducting dome, for example, evolving from magnetic- to orbital-fluctuation mediated superconductivity [28–30]. Alternatively, the gap can become progressively more anisotropic within the same universal pairing scenario based on competing inter-band coupling and intra-band Coulomb repulsion and pair-breaking impurity scattering [31, 32].

In conclusion, the London penetration depth, $\lambda(T)$, was measured in single crystals of $Ca_{10}(Pt_3As_8)[(Fe_{1-x}Pt_x)_2As_2]_5$ (10-3-8) with different levels of Pt-doping, x. T_c increases monotonically reaching 10.5 K for $x = 0.097$. The power-law fit to the low temperature part of $\Delta\lambda(T)$ shows that the average exponent, n_{avg}, varies from 2.36 to 1.7, which can be explained by an increasing anisotropy of the superconducting gap at the edges of the superconducting dome. This behavior is not a consequence of the coexistence of superconductivity and magnetism or high electronic anisotropy. It is a universal and robust property of iron pnictide superconductors and, most likely, comes from the multiband physics of the superconducting pairing.

We thank Andrey Chubukov and Peter Hirschfeld for useful discussions. Work at the Ames Laboratory was supported by the Department of Energy-Basic En-

* Corresponding author: prozorov@ameslab.gov

[1] M. Nohara, S. Kakiya, and K. Kudo, Proceedings of the International Workshop on Novel Superconductors and Super Materials, a-41 (2011).

[2] S. Kakiya, K. Kudo, Y. Nishikubo, K. Oku, E. Nishibori, H. Sawa, T. Yamamoto, T. Nozaka, and M. Nohara, J. Phys. Soc. Japan **80**, 093704 (2011).

[3] N. Ni, J. M. Allred, B. C. Chan, and R. J. Cava, Proceedings of the National Academy of Sciences **108**, E1019 (2011).

[4] C. Lohnert, T. Sturzer, M. Tegel, R. Frankovsky, G. Friederichs, and D. Johrendt, Angew. Chem. Int. Ed. **50**, 9195 (2011).

[5] M. Neupane, C. Liu, S.-Y. Xu, Y. J. Wang, N. Ni, J. M. Allred, L. A. Wray, H. Lin, R. S. Markiewicz, A. Bansil, R. J. Cava, and M. Z. Hasan, arXiv:1110.4687 (2011).

[6] M. M. Altarawneh, K. Collar, and C. H. Mielke, Phys. Rev. B **78**, 220505 (2008).

[7] M. Putti, I. Pallecchi, E. Bellingeri, M. R. Cimberle, M. Tropeano, C. Ferdeghini, A Palenzona, C. Tarantini, A. Yamamoto, J. Jiang, J. Jaroszynski, F. Kametani, D. Abraimov, A. Polyanskii, J. D. Weiss, E. E. Hellstrom, A. Gurevich, D. C. Larbalestier, R. Jin, B. C. Sales, A. S. Sefat, M. A. McGuire, D. Mandrus, P. Cheng, Y. Jia, H. H. Wen, S. Lee, and C. B. Eom, Supercond. Sci. Technol. **23**, 034003 (2010).

[8] A. Gurevich, Rep. Prog. Phys. **74**, 124501 (2011).

[9] R. Prozorov, M. A. Tanatar, N. Ni, A. Kreyssig, S. Nandi, S. L. Bud'ko, A. I. Goldman, and P. C. Canfield, Phys. Rev. B **80**, 174517 (2009).

[10] N. Plakida, "High-Temperature Cuprate Superconductors: Experiment, Theory, and Applications", 1st ed., Springer Series in Solid-State Sciences, Vol. **166**, p.570 (2010).

[11] R. Prozorov and V. G. Kogan, Rep. Prog. Phys. **74**, 124505 (2011).

[12] H. Kim, M. A. Tanatar, B. Shen, H.-H. Wen, and R. Prozorov, arXiV:1105.2265 (2011).

[13] R. T. Gordon, H. Kim, N. Salovich, R. W. Giannetta, R. M. Fernandes, V. G. Kogan, T. Prozorov, S. L. Bud'ko, P. C. Canfield, M. A. Tanatar, and R. Prozorov, Phys. Rev. B **82**, 054507 (2010).

[14] R. Prozorov and R. W. Giannetta, Supercond. Sci. Technol. **19**, R41 (2006).

[15] C. T. Van Degrift, Rev. Sci. Instrum. **46**, 599 (1975).

[16] R. Prozorov, R. W. Giannetta, A. Carrington, and F. M. Araujo-Moreira, Phys. Rev. B **62**, 115 (2000).

[17] M. A. Tanatar, A. Kreyssig, S. Nandi, N. Ni, S. L. Bud'ko, P. C. Canfield, A. I. Goldman, and R. Prozorov, Phys. Rev. B **79**, 180508 (2009).

[18] E. Salje, B. Kuscholke, and B. Wruck, Phys. Chem. Minerals **12**, 132 (1985).

[19] Unpublished data obtained from private communication with N. Ni. At $x = 0.004$, structural transition of $T_s \sim 90$ K was observed in resistivity.

[20] M. A. Tanatar, J.-Ph. Reid, H. Shakeripour, X. G. Luo,

N. Doiron-Leyraud, N. Ni, S. L. Bud'ko, P. C. Canfield, R. Prozorov, and L. Taillefer, Phys. Rev. Lett. **104**, 067002 (2010).

[21] J.-Ph. Reid, M. A. Tanatar, X. G. Luo, H. Shakeripour, N. Doiron-Leyraud, N. Ni, S. L. Bud'ko, P. C. Canfield, R. Prozorov, and L. Taillefer, Phys. Rev. B **82**, 064501 (2010).

[22] S. L. Bud'ko, N. Ni, and P. C. Canfield, Phys. Rev. B **79**, 220516 (2009).

[23] D. C. Johnston, Advances in Physics **59**, 803 (2010).

[24] V. G. Kogan, C. Martin, and R. Prozorov, Phys. Rev. B **80**, 014507 (2009).

[25] R. T. Gordon, H. Kim, M. A. Tanatar, R. Prozorov, and V. G. Kogan, Phys. Rev. B **81**, 180501 (2010).

[26] T. Nakano, S. Tsutsumi, N. Fujiwara, S. Matsuishi, and H. Hosono, Phys. Rev. B **83**, 180508 (2011).

[27] H. Luetkens, H.-H. Klauss, M. Kraken, F. J. Litterst, T. Dellmann, R. Klingeler, C. Hess, R. Khasanov, A. Amato, C. Baines, M. Kosmala, O. J. Schumann, M. Braden, J. Hamann-Borrero, N. Leps, A. Kondrat, G. Behr, J. Werner, and B. Buchner, Nature Materials **8**, 305 (2009).

[28] H. Kontani and S. Onari, Phys. Rev. Lett. **104**, 157001 (2010).

[29] S. Onari, H. Kontani, and M. Sato, Phys. Rev. B **81**, 060504 (2010).

[30] T. Saito, S. Onari, and H. Kontani, Phys. Rev. B **82**, 144510 (2010).

[31] A. V. Chubukov, Annu. Rev. Condens. Matter Phys. **3**, null (2012).

[32] P. J. Hirschfeld, M. M. Korshunov, and I. I. Mazin, Rep. Prog. Phys. **74**, 124508 (2011).